Simulation and Tolerance Study of XUV and Soft X-rays Pulse Shaper

Author: Ali Raza

Supervisor: Leslie Lamberto Lazzarino

Ali Raza   *Simulation and Tolerance Study of XUV and Soft X-rays Pulse Shaper* ,

Summer Student Program

X-Rays Femotchemsitry Group

Photon Science Department

DESY, Hamburg, Germany.

Supervisor   *Leslie Lamberto Lazzarino*

Introduction

1.1 Pulse Shaping

Since the advent of the laser, there has been a sustained interest in generating ultrashort laser pulses in the picosecond and femtosecond range. Over the past two decade powerful optical waveform synthesis or pulse shaping methods have been developed which allow generation of complicated ultrafast optical waveforms according to user specification. Coupled with the recent advances and resulting widespread availability of femtosecond lasers, as well as advances in femtosecond pulse characterization techniques, femtosecond pulse shaping is poised to impact many diverse and additional applications. For many applications it is desirable and necessary to modify the pulses from the source in a well-defined manner. Pulse shaping is the process of changing the waveform of transmitted pulses [1, 2]. On a fs time scale, many interactions depend on the particular temporal shape of the waveform being applied. One widely uses technique involves pump probe spectroscopy to investigate the temporal dynamics of molecules and atoms in laser fields. This pump probe spectroscopy has been used, for example, to study the interaction of ionic wave packets [3, 4], the polarization of high harmonic generation [5] and the tomographic reconstruction of the highest occupied molecular orbital of nitrogen [6]. Another widely used technique is sinusoidal spectral phase modulation. Sinusoidal spectral phases have been utilized to control and investigate wave packet dynamics of polyatomic molecules and atoms [7, 8].

There exists different types of basic pulse shaper, for example, Michelson Interferometer producing two pulses with certain delay, grating compressor, chirped

mirror etc. Here we concentrate on more widely used pulse shaping technique which is waveform synthesis by spatial masking of the spatially dispersed optical frequency spectrum. This is achieved by introducing the mask in the focal plane of a free dispersion line which is also called 4−f device as shown in Fig. 1.1. This design was presented by Froehly and co-workers [9] in 1983.

A zero dispersion line composed of a pair of grating and lenses (or curved mirrors), arranged in a 4f set-up. The input light beam is spectrally dispersed in different angles by the first grating and focused by the first lens/mirror at fourier plane. Then a second combination of lens (or curved mirror) and grating allows the recombination of all the frequencies into a single collimated beam [1]. If nothing is placed at the focal plane then the output light will be exactly the same as input only the amplitude will be decreased due to limited grating transmission. By putting a specific mask at the focal plane, optical path length or the optical density of each spectral component can be modified hence beam can be shaped.

Depending on the mask type, a 4f pulse shaper can control both phase and amplitude, the polarization and also the transverse spatial profile. [10]. Some examples of different kind of masks are e.g micro mirror Array(MMA), liquid crystal phase modulators array and acousto-optic deflector. Micro mirror array is the array of mirrors placed two dimensionally as shown in Fig. 1.2. Each individual mirror can be tilted along any of the axis and can be moved independently.
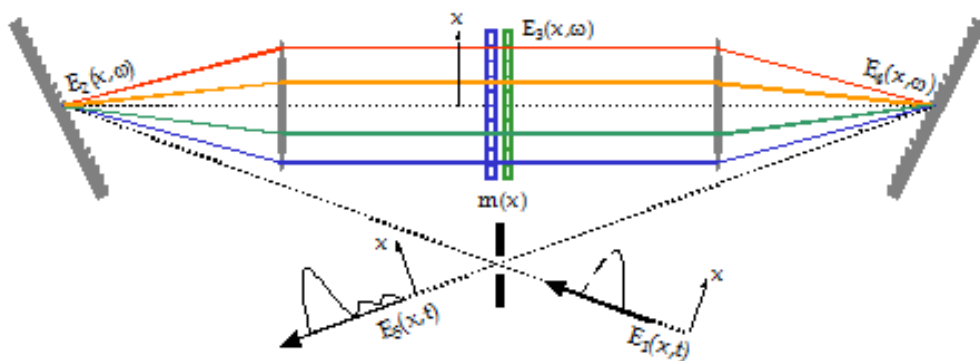
Figure 1.1: Schematic of 4-f pulse shaper [2].

2
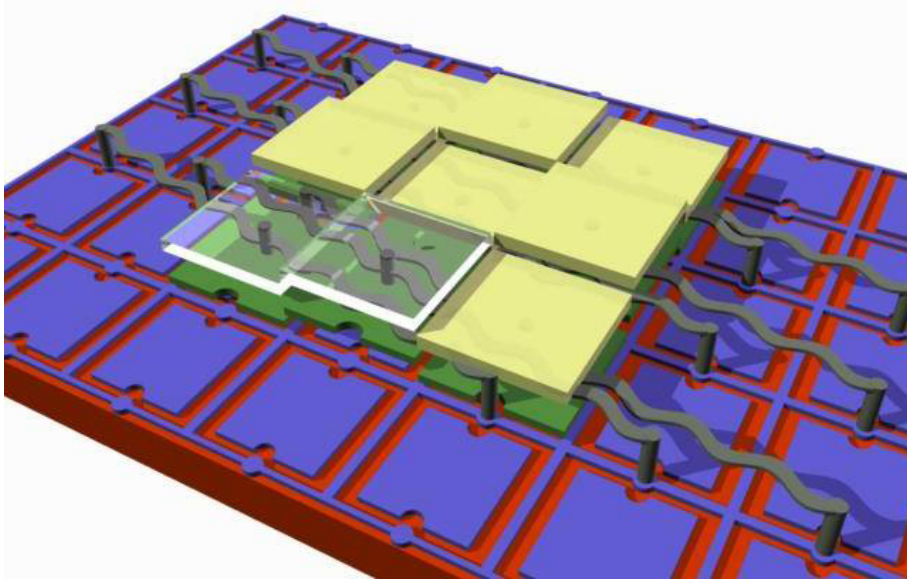
Figure 1.2: Micro mirror assembley.

1.2   XUV & Soft X-Rays pulse shaping

XUV and soft X-Rays cover the EM spectrum from 0.2nm to 40nm. The pulse shaper we intend to develop will work in the spectral range from 40nm and 4nm, covering the whole XUV spectrum and part of the soft X-rays spectrum. Compression of these femtosecond pulses has a lot of applications e.g. soft X-rays excite atom electrons in the inner shells which gives element specific information about different elements in a compound and it also helps to detect structural changes of atom. Pulse compression with 4f geometry is widely used for visible light and that technology can be effectively transferred to soft X-Rays. But it faces a lot of challenges e.g. we cannot use the mirrors/lenses at normal incident due to poor transmission of XUV and soft X-rays. To solve this problem mirror coated with carbon or nickel, at shorter wavelengths, are used. The gratings available don't have high overall efficiency (Grating efficiency + tramsmitivity) e.g molybdenum has 10% efficiency at 13.4nm wavelength.

Simulation and of XUV−Soft X-Rays beam shaper

2.1 Zemax model of pulse shaper

In this section, the Zemax simulation of pulse shaper (4-f geometry) is presented. As shown in Fig. 2.1, only lenses are replaced by the mirrors to increase the transmission. Two external mirrors, M1 and M4, are placed before and after the 4-f geometry to focus the beam transversely with respect to the plane where device works. The light diffracted by grating G1 to different angles is focused on the MMA by the mirror M2. After inducing the phase variation by the MMA on these different spectral components, the mirror M3 and grating G2 combine them back in a single beam. All form of mirrors are cylindrical.

In hybrid model, geometry is exactly the same, only the sequential grating is replaced by the non sequential grating.

2.2 System Specification

In this section, system specifications i.e. the distance "f" of 4-f geometry, grazing incidence angles, coating of the mirror etc, are presented.

Beam shaper is designed for the XUV and soft X-Rays: wavelengths of particular interests are 38nm(fundamental harmonic for sFLASH), 12.4nm ($3^{r}d$ harmonic of 38nm)and 4.3nm (carbon K-edge). For the free - standing gratings in hybrid mode, two material are tested, molybdenum and Niobium. In the wavelength range of our interest, gratings made with either material show a similar transmission with a minimum of 2% and a maximum of 4%. The distance "f" of the 4-f geometry and distance between grating and external focusing mirror on both sides is 300mm each
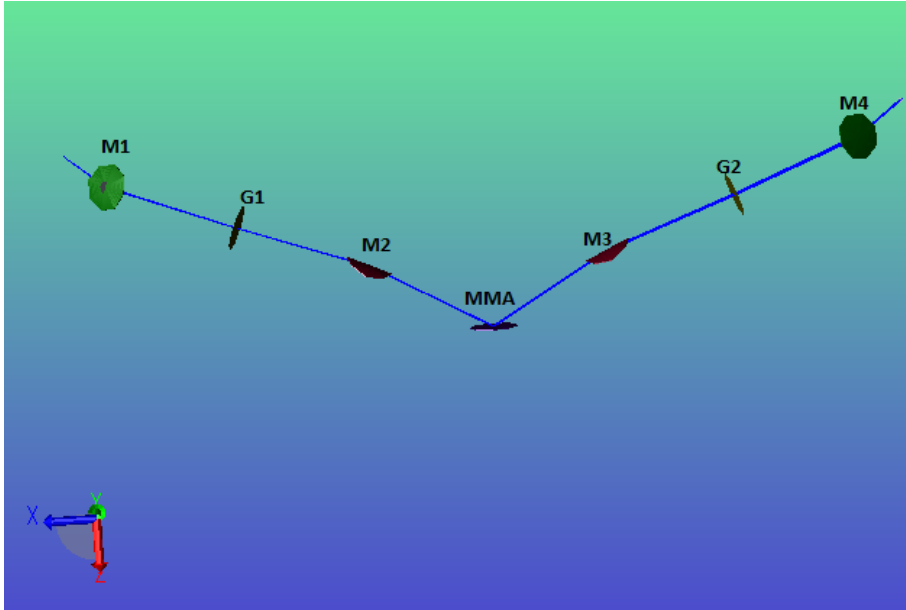
Figure 2.1: Zemax sequential 3.D model of pulse shaper. Here angles and distances have been chosen randomly only for illustration purposes.

and The grazing angle is kept at $5\,^\circ$.

For the mirror coatings, two types of material are selected, carbon and nickel. As shown in Fig. 2.2, for the wavelength above 6nm the reflectivity of carbon is above 80% while there is abrupt decrease at lower wavelength, while that of nickel, the reflectivity is around 60% through out in XUV and soft X-Rays range as shown in Fig. 2.3.

C 200.nm on SiO2 at 5.deg, P=0.

Reflectivity

Wavelength (nm)
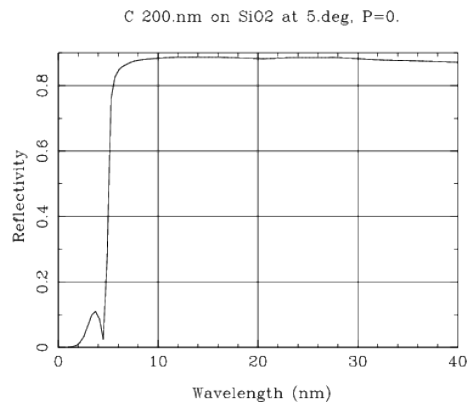
Figure 2.2: Reflectivity of carbon coated Si mirror. [11]

Ni 200.nm on SiO2 at 5.deg, P=0.

Reflectivity

Wavelength (nm)
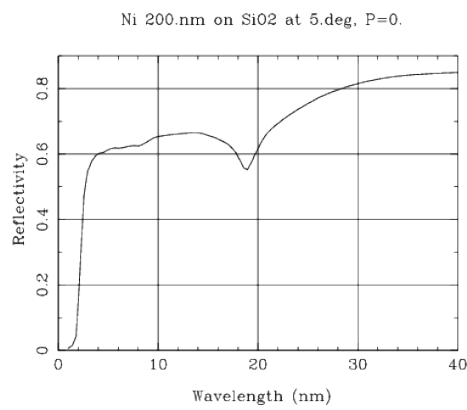
Figure 2.3: Reflectivity of nickel coated Si mirror. [11]

Results & Discussions

In this chapter, the results from simulation has been briefly discussed. Zemax hybrid mode (sequential + non.sequential) is used to construct the molybdenum grating: all the parts except gratings are made in sequential mode while gratings are simulated as non sequential component. First the resolution of the system obtained using this grating is calculated then the divergence of the source has been varied and resulting divergence has been computed. In the end, the mechanical tolerances of each optical component are estimated.

As shown in Table.3.1, the resolution of the pulse shaper is 47500 at 38nm wavelength and 0.233 mrad source divergence. The spot diagram at the output plane and at the fourier plane (MMA) are shown in Fig. 3.2 and Fig. 3.2 respectively. We can see the lines at MMA are well focused, giving higher resolution.

TABLE 3.1

Resolution of beam shaper with 90nm thick and 5000 lines/mm molybdenum grating. Divergence of beam is 0.233 mrad

λ(nm)	n_{Mo}	R_{Mo}
38	0.90	47500
12.7	0.93	8670
4.3	0.995	2600

The effect of divergence on resolution of the beam shaper and new focus distance of the 4-f geometry is shown in Table.3.2. The half angle divergence of 0.233 mrad giving 47500 resolution is the one at which the whole system is optimized. We can
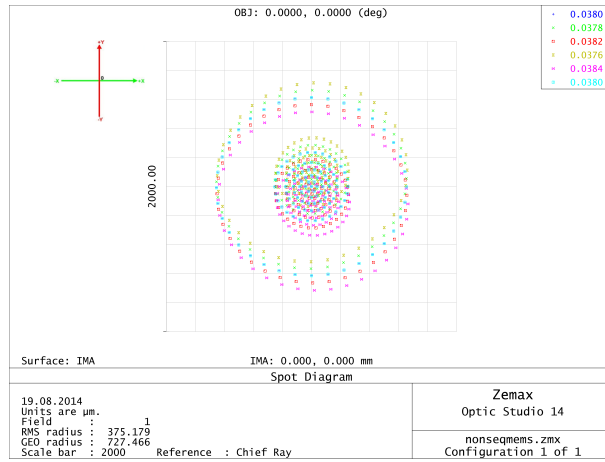
Figure 3.1: Spot diagram at output plane.
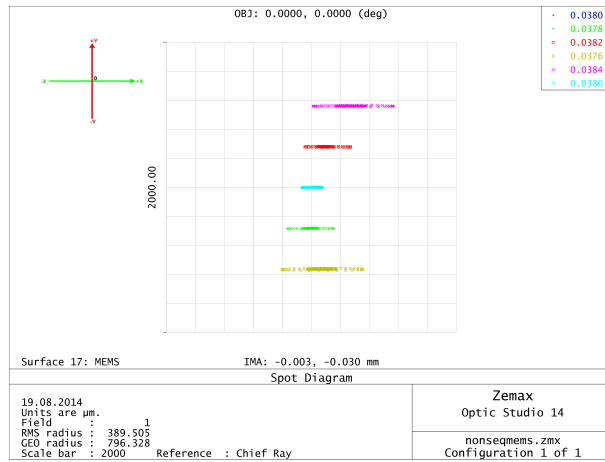
Figure 3.2: Spot diagram at fourier plane.

see the resolution decreases as we increase or decrease divergence. The focusing distance f is increasing as the divergence increases. As expected, some weird results come when we move far away from the optimized half angle divergence (e.g. ten times that of optimized value) of the source as shown in Fig. 3.3 and Fig. 3.4.

TABLE 3.2

Effect of different divergences on resolution and f distance of 4-f geometry. Θ, f and R are the half angle divergence, focal distance of 4-f geometry and resolution of pulse shaper.

Θ (mrad)	f (mm)	R
0.117	290	10860
0.175	295	38000
0.233	300	47500
0.467	315	15200
0.933	335	10860
1.630	350	07600
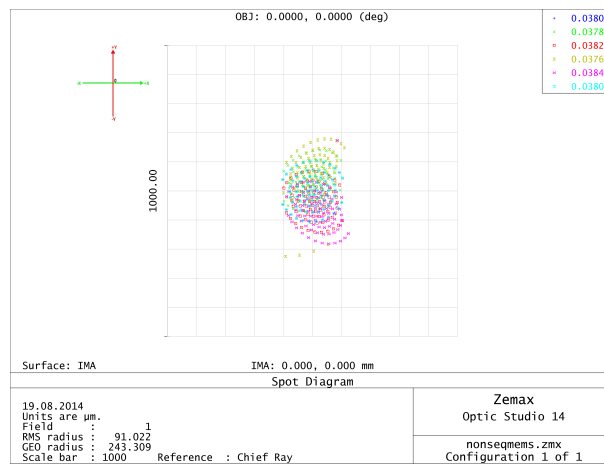
Figure 3.3: Spot diagram at output plane when beam divergence is 1.630 mrad.

The mechanical tolerances of each component in the pulse shaper are listed in the Table.3.2. Tolerances for all the six dimensions of each component are obtained by fixing five coordinates and varying one. As we can see in the table some positions

9
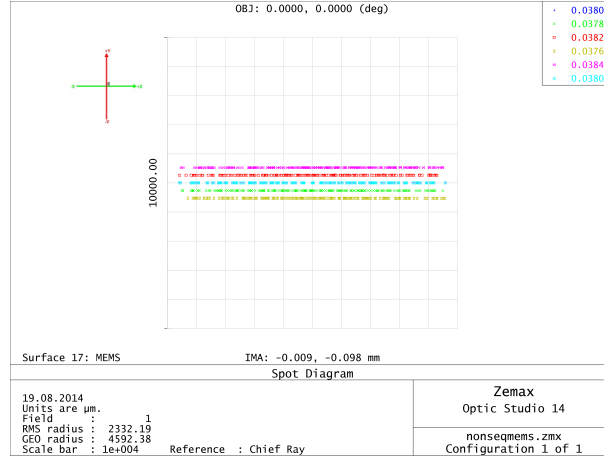
Figure 3.4: Spot diagram at fourier plane when beam divergence is 1.630 mrad.

like y.tilt of MMA, z.tilt of mirror M3, z.tilt of mirror M1 etc. are very crucial and need special attention in engineering the device.

TABLE 3.3

Mechanical Tolerances of each component of the pulse shaper. All the lengths and angles are in mm and degree respectively. All components like M1, G1, M2 are shown in Fig. 2.1.

Surface	L_x	L_y	L_z	Θ_x	Θ_y	Θ_z
M1	-0,1 to 0,1	-1 to 1	-1 to 1	-0,01 to 0,01	-0,1 to 0,1	-0,01 to 0,01
G1	-1 to 1	-1 to 1	-0,01 to 1	-1 to 1	-1 to 1	-0,1 to 0,1
M2	-1 to 1	-0,5 to 0,5	-1 to 1	-0,5 to 0,5	-0,01 to 0,01	-0,01 to 0,01
MMA	-1 to 1	-1 to 1	-0,1 to 0,1	-0,5 to 0,5	-0,01 to 0,01	-1 to 1
M3	-1 to 1	-0,1 to 0,1	-1 to 1	-0,5 to 0,5	-0,05 to 0,05	-0,05 to 0,05
G2	-1 to 1	-1 to 1	0 to 1	-1 to 1	-1 to 1	-0,5 to 0,5
M4	-1 to 1	-1 to 1	-1 to 1	-0,1 to 0,1	-1 to 1	-0,05 to 0,05

The effect of combined different tolerances on spot size is shown in Fig. 3.5 and Fig. 3.6. The resolution of pulse shaper under the combined different tolerances is 10860. We can see in right small window of Fig. 3.6 that the lines at $\lambda = 38$nm and $\lambda = 38.0014$nm, reported with all elements perfectly aligned, are now overlapped

because they are unfocused and that results in low resolution.
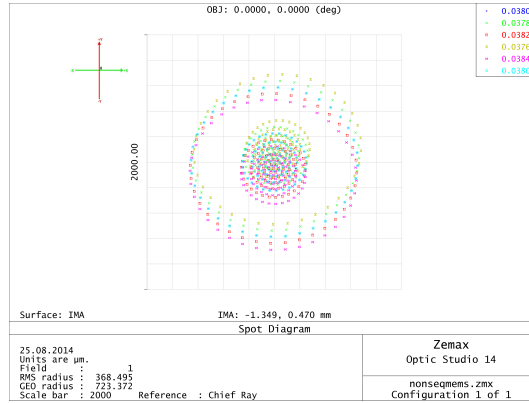
Figure 3.5: Effect of combined tolerances on spot size at output plane.
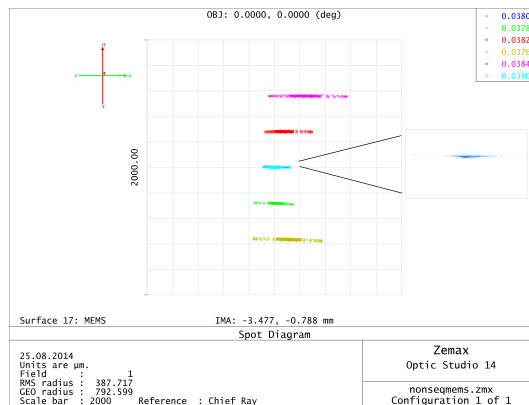
Figure 3.6: Effect of combined tolerances on spot size at fourier plane.The right small window is the zoomed version of spot size at $\lambda = 38$nm.

Conclusion

In this project 4-f beam shaper for XUV and soft X-rays is simulated in Zemax software. In the construction of 4-f geometry, molybdonium grating and cylindrical mirrors are used. The optimized design reaches a 47500 resolution at 38nm wavelength with a 0.233mrad half angle divergence. The effects of different beam divergences are studied. The alignment tolerances of each optical components are estimated and presented in tabulated form.

[1] M. Grishin, *Advances in Solid State Lasers Development and Applications* (InTech, 2010).

[2] J. Diels and W.Rudolph, *Ultrashort Laser Pulse Phenomena*, 2nd ed. (Elsevier Inc, 2006).

[3] D. Geissler, B. J. Pearson, and T. Weinacht, "Wave packet driven dissociation and concerted elimination in $CH2I2$," *J. Chem. Phys.* **127**, 204305 (2007).

[4] B. J. Pearson, S. R. Nichols, and T. Weinacht, "Molecular fragmentation driven by ultrafast dynamic ionic resonances," *J. Chem. Phys.* **127**, 131101 (2007).

[5] X. Zhou, R. Lock, N. Wagner, H. C. Kapteyn, and M. M. Murnane, "Elliptically polarized high-order harmonic emission from molecules in linearly polarized laser fields," *Phys. Rev. Lett.* **102**, 73902 (2009).

[6] J. Itatani, J. Levesque, D. Zeidler, H. Niikura, H. Pépin, J. C. Kieffer, P. B. Corkum, and D. M. Villeneuve, "Tomographic imaging of molecular orbitals," *Phys. Rev. Lett.* **432**, 867–871 (2004).

[7] R. Selle, T. Brixner, T. Bayer, M. Wollenhaupt, and T. Baumert, "Modelling of ultrafast coherent strong-field dynamics in potassium with neural networks," *J. Phys. At. Mol. Opt. Phys.* **41**, 074019 (2008).

[8] N. Dudovich, D. Oron, and Y. Silberberg, "Single-pulse coherent anti-Stokes Raman spectroscopy in the fingerprint spectral region," *J. Chem. Phys.* **118**, 9208 (2003).

[9] C. Froehly, B. Colombeau, and M. Vampouille, "Shaping and analysis of picosecond light pulses," *Prog. opt.* **20**, 65–153 (1983).

[10] T. Feurer, J. C. Vaughan, R. M. Koehl, and K. A. Nelson, "Multidimensional control of femtosecond pulses by use of a programmable liquid-crystal matrix," *Opt. Lett.* **27**, 652–654 (2003).

[11] Layered Mirror Reflectivity, www-page, http://henke.lbl.gov/optical_constants/layer2 .html (valid 02.09.2014).